

CERN-EP/79-05
22 January 1979

A LARGE SUPERCONDUCTING DIPOLE
COOLED BY FORCED CIRCULATION OF TWO-PHASE HELIUM

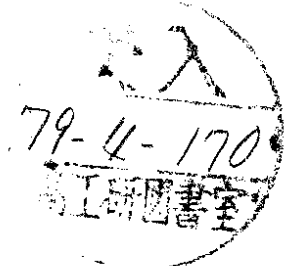
M. Morpurgo

CERN, Geneva, Switzerland

ABSTRACT

A large superconducting dipole cooled by forced circulation of two-phase helium is described. Details are given of the magnet design and construction. There follow a short discussion of some cryogenic problems and the first results from the dipole operation.

(Submitted to Cryogenics)



1. GENERAL

A superconducting dipole cooled by forced circulation of two-phase helium has been constructed.

Figure 1 gives a general view of the magnet, which is installed at CERN in a high-energy particle beam of the 300 GeV Proton Synchrotron. The main characteristics of the dipole are:

Central maximum field	1.9 T
Free warm bore	1.6 m
Over-all length	3.5 m
Weight of the cold part of the magnet	≈ 40 t
Over-all weight	230 t
Maximum current	6000 A
Stored energy	≈ 20 MJ

The magnet is wound with a hollow composite superconductor, through which two-phase helium is circulated by means of cold reciprocating pumps.

The dipole was put into operation in June 1978 and has worked since, almost without interruption.

The dipole was designed at CERN. The composite hollow superconductor and pump circulating system were also manufactured at CERN. Iron yoke, refrigerator, and coils were manufactured respectively by the firms Thyssen (Germany), Sulzer (Switzerland), and Ansaldo (Italy). The cost of the dipole, not including the refrigerator, was ≈ 5 MSF.

2. MAGNET DESCRIPTION

2.1 General

The dipole consists essentially of two saddle-shaped coils, which are mounted inside a cylindrical bore in the iron yoke (see Fig. 2). The iron yoke has the double purpose of enhancing the central field and reducing the external stray field. The geometry of the saddle-shaped coils is relatively simple, yet it gives

a fairly uniform field distribution in the useful region of the magnet. The field variation in the central plane of the magnet is approximately $\pm 5\%$.

2.2 Conductor and coils

The two coils are wound with a hollow composite superconductor of square cross-section 18×18 mm with a central bore of diameter 10 mm (Fig. 3). The composite superconductor consists of a central copper pipe on which a number of standard superconducting Nb-Ti wires [produced by the firms IMI (Great Britain) and BBC (Switzerland)] are cabled. The cable is sandwiched between two copper profiles (Fig. 4) and the resulting composite is soft-soldered, in a single operation, by means of a tin-silver alloy. The manufacturing process is very similar to the one described in an earlier paper¹⁾.

Each saddle-shaped coil consists of 10 layers having 30 turns each. The conductor length required varies between 240 and 270 m per layer. The layers are wound, one on top of the other, on a cylindrical mandrel. The mandrel is free to oscillate around its horizontal axis and is mounted on a turning table with vertical axis. The conductor is insulated by wrapping it over its entire length with two half-overlapped glass tapes. Electrical connections of layers are made by overlapping, mechanically clamping, and soft-soldering the end sections of adjacent layers. After having wound the ten layers, each coil was given its exact final shape by tightening it into a mould which was subsequently used to impregnate the coil, under vacuum, with an epoxy resin.

2.3 Coil-supporting structure

The two saddle-shaped coils (item 1 on Fig. 5) are mounted onto an inner stainless steel cylinder (2), onto which they are clamped by means of two outer half-cylinders (3) and tie bolts (4). The combination of the inner and outer cylinders and of the coils results in a structure capable of withstanding the very considerable electromagnetic forces acting on the windings. The complete assembled coil is suspended in a soft steel cylinder (5) (which is at the same time vacuum tank and part of the iron yoke) by means of 8 titanium alloy rods (7). These rods should support only the coil weight if the coil was perfectly centred with respect

to the iron yoke. In practice the rods must also be designed to withstand the stresses arising from a possible eccentricity in the coil positioning. Horizontal titanium rods (6) are used to withstand horizontal forces.

3. DIPOLE CRYOGENICS

3.1 General

Figure 6 shows a schematic diagram of the helium flow. In normal operation two reciprocating pumps ensure a total flow of approximately 150 g/s of two-phase helium through the twenty parallel circuits into which the magnet is subdivided. The two pumps are connected in parallel by means of cold non-return valves to make sure that, if one pump fails, the second one will maintain a certain helium flow through the magnet. A description of the pump is given in an earlier paper²⁾. The pressure drop in the magnet is approximately 180 g and the corresponding helium velocity in the hollow superconductor is ≈ 0.75 m/s.

3.2 Choice of the cooling scheme

It was considered desirable to make the dipole operation independent of the refrigerator plant. This justifies the use of pumps to circulate the helium. However, pumps introduce in the magnet system an extra cryogenic loss $W = f \cdot \Delta p / \eta$, where f , Δp , and η are, respectively, the volumetric helium flow, the pressure drop, and the pump efficiency. For a given flow f the only possibility to reduce the losses is to keep the pressure drop Δp small. However, a small Δp corresponds, generally, to small helium velocity, which yields, in the case of supercritical helium, a poor heat exchange coefficient between helium and the conductor wall. On the contrary, in the case of two-phase helium, where nucleate boiling can occur, the heat exchange is good even at very low or zero helium velocity. A more detailed analysis of the helium thermodynamic cycle (Fig. 7) shows that, in the scheme used, subcooled helium is circulated in the first section of the coil (between points A and B), while two-phase helium is circulated only in the second section of the coil (between points B and C). Measurements³⁾ have shown that the heat exchange coefficient is also high in the case of subcooled helium at zero velocity.

A serious problem with two-phase helium arises from the possibility of having liquid and vapour separation. In this case it could happen that sections of conductor, cooled only by vapour, would cause a coil quenching. Baker's diagram⁴⁾ should allow the flow régime in the magnet circuit to be determined. However, results given by this diagram should be taken with some caution. The first operation of the dipole has shown evidence of phase separation, although the operating point was well inside the bubble or froth region. Apparently, a certain amount of helium vapour was slowly accumulating somewhere in the magnet. After some time, the accumulated vapour was suddenly discharged, causing the magnet quenching. The phenomenon was cyclic with a period of several hours. To avoid phase separation it was necessary to increase the helium velocity in the conductor from the original design figure of 0.5 m/s up to 0.75 m/s.

A second problem, which should be considered in the case of several parallel circuits cooled by two-phase helium, is the possibility of instabilities in the flow distribution.

It is commonly claimed that instabilities are originated by the fact that the hydraulic impedance of a circuit is a rising function of the helium quality (i.e. the higher the vapour content in the circulating helium, the higher the circuit impedance).

A heat source in one of the circuits will raise the helium quality factor. This will decrease the flow, again raising the quality factor and leading, eventually, to a situation where only vapour circulates in the heated circuit. In practice, we have not experienced any difficulties due to flow instabilities, which, in our opinion, can be avoided by a proper design.

Figure 8 shows an experimental curve (full line), where the helium flow in a given pipe for a given pressure drop is plotted against the vapour quality. Flow becomes unstable when $X \geq 0.75$. The experimental curve corresponds fairly well with the curve calculated according to a modified version⁵⁾ of Martinelli's theory. The dotted curve in Fig. 8 represents the power which can be generated

at the pipe inlet, assuming that the pipe is fed by liquid helium ($X = 0$). This curve has a maximum W_m for $X \approx 0.75$. To avoid flow instabilities in parallel circuits, it is necessary to evaluate the maximum heating power which is generated in each circuit and make sure that this heating power is much lower than W_m .

3.3 Cooling down

The initial cooling down of the magnet from room temperature is made by circulating the helium coming out from the refrigerator directly through the coil. This requires setting the double valve V (Fig. 6) in the appropriate position. During cooling down the temperature difference between the coldest and the warmest points of the coil was always ≤ 30 K.

When the magnet is cold, liquid helium is produced in the cryostat. When this is filled, valve V is switched onto its second position and the pumps are started. The refrigerator liquefies directly in the cryostat, and pumps provide the helium circulation through the magnet.

The cooling-down time, starting from room temperature, is ≈ 10 days. This time may appear very long but, in practice, it is not a serious inconvenience because this operation is repeated very rarely. When the magnet is not used and the refrigerator is stopped, the warming up rate of the coils is very low. Therefore after an operation interruption of, say, one month, the magnet temperature will only rise up to 100 K and recooling of the magnet from that temperature will be fairly fast.

4. CONCLUSIONS

The construction of this dipole has shown the feasibility of magnets cooled by forced circulation of two-phase helium. The major design difficulty of this technique seems to be predicting when phase separation occurs. Phase separation depends on many parameters, such as helium velocity, circuit geometry, and heat input in the circuit.

The advantages of two-phase helium are the high exchange coefficient, the high heat-absorbing capacity without temperature variation, and the simplicity of the system.

Acknowledgements

A great many people have taken part in this work and their contributions are very gratefully acknowledged. In particular, the author would like to thank M. Marquet and his technicians who have taken care of the mounting of the cryogenic system; J.-P. Grillet who surveyed the yoke construction and contributed with magnetic field computer calculations; T. Goiffon who carried out the majority of the drawing work; P. Gorce, M.-N. Grossi and H. Piney who assisted in the dipole mounting; A. Cyvoct and A. Renoux who were in charge of the magnet power supply and controls; G. Pozzo and C. Rosset to whom is due the fabrication of the composite superconductor.

The author is much indebted to F. Schmeissner and to F. Birchler and J.-P. Dauvergne and their staff who took care of the refrigeration system.

Finally, many thanks are due to Mr. Odaglia and to the staff of the firm Ansaldo who contributed to solving several fabrication problems.

REFERENCES

- 1) M. Morpurgo and G. Pozzo, Fabrication of an aluminium stabilized superconductor, Cryogenics 17, 87 (1977).
- 2) M. Morpurgo, Design and construction of a pump for liquid helium, Cryogenics 17, 91 (1977).
- 3) E.A. Ibrahim, R.W. Boom and G.E. McIntosh, Heat transfer to subcooled liquid helium, Advances in Cryogenic Engng. 23, 333 (1978).
- 4) M.A. Green, Determination of the safe operating point for the hydraulic operation of the magnets and the transfer lines, Lawrence Berkeley Lab. Engineering note, 2 August 1976.
- 5) M. Firth, CERN, private communication.

Figure captions

- Fig. 1 : General layout of the dipole and of the cooling system.
- Fig. 2 : Coil geometry.
- Fig. 3 : Composite superconductor cross-section.
- Fig. 4 : Exploded view of the superconductor.
- Fig. 5 : Dipole cross-section.
- Fig. 6 : Schematic diagram of helium flow.
- Fig. 7 : Helium thermodynamic cycle.
- Fig. 8 : Helium flow in a pipe for a given pressure drop as a function of helium quality.

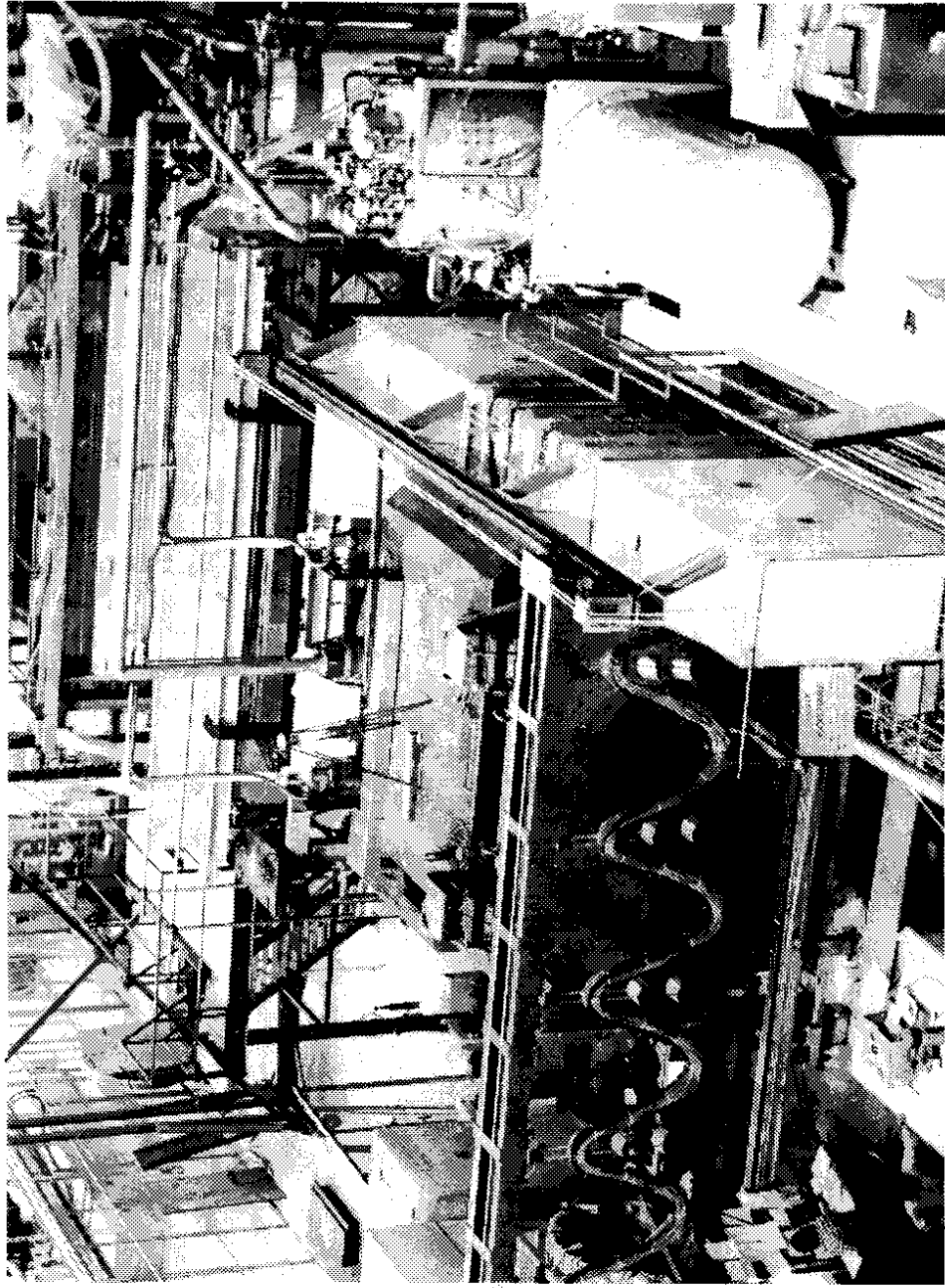


Fig. 1

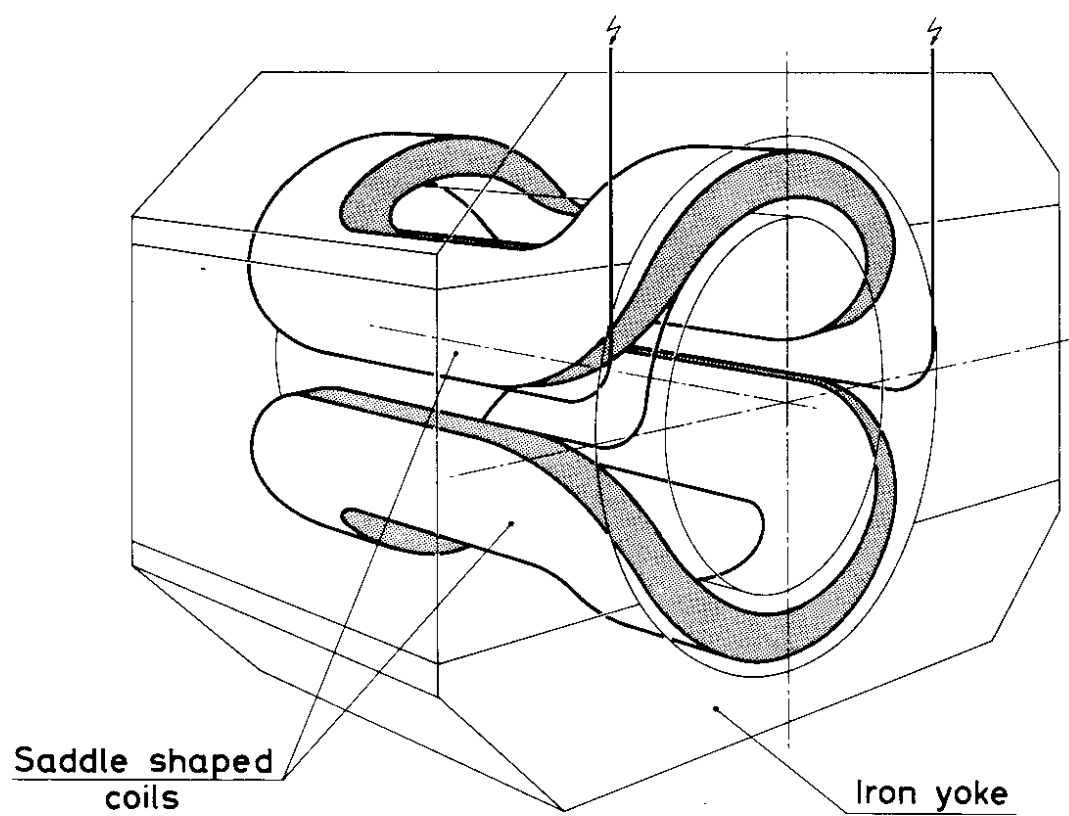


Fig. 2

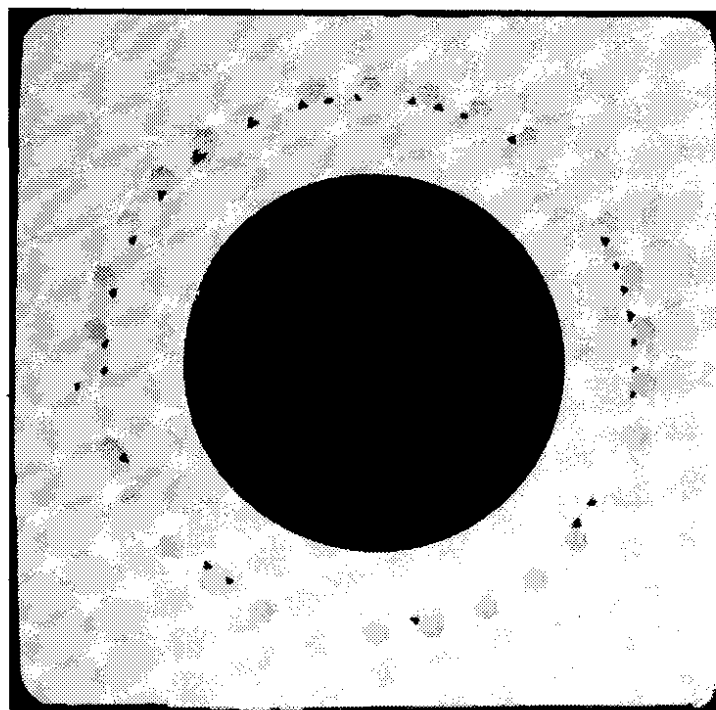


Fig. 3

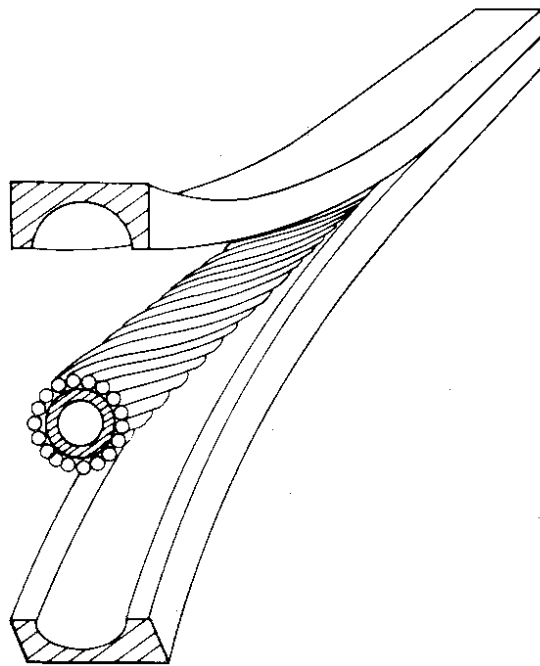


Fig. 4

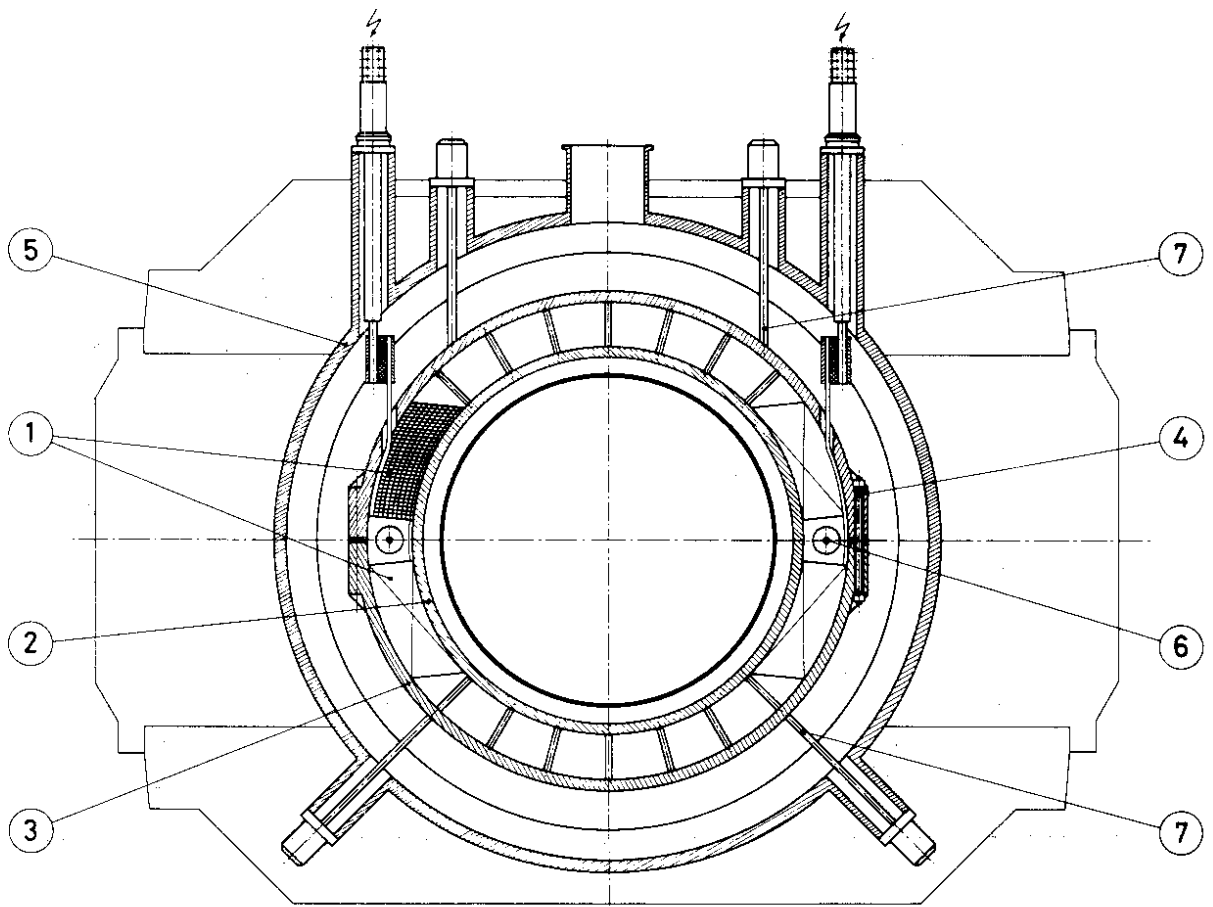


Fig. 5

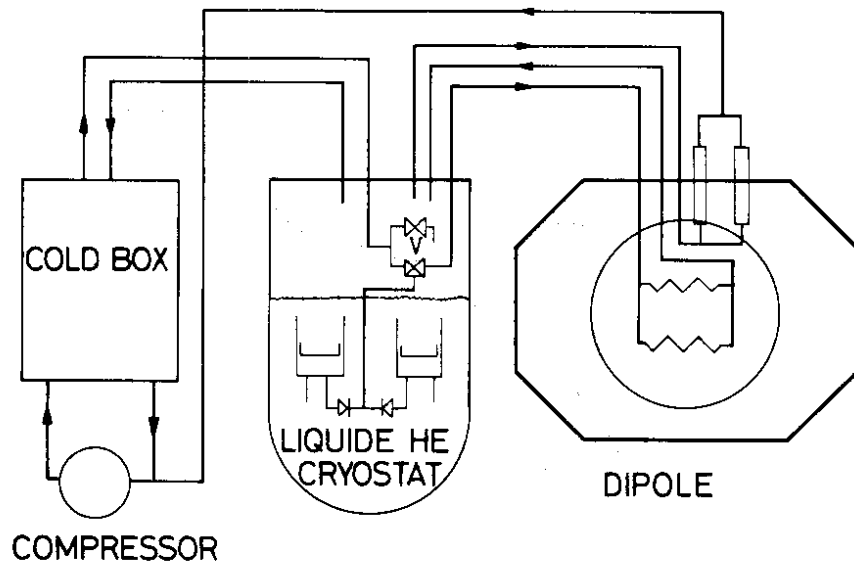


Fig. 6

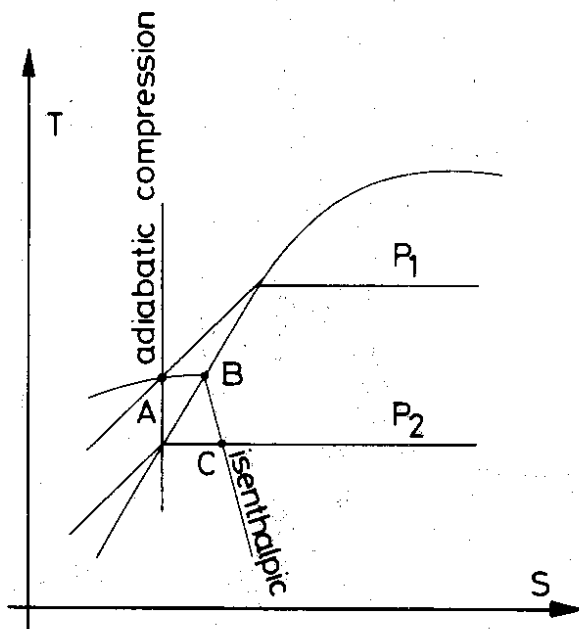


Fig. 7

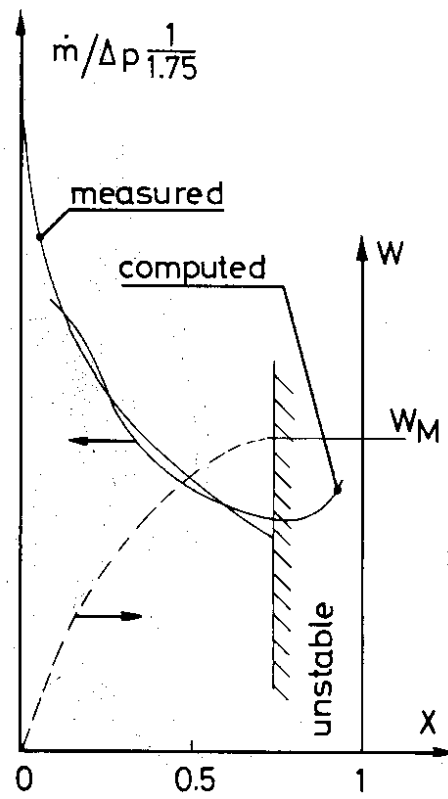


Fig. 8